

53. SEDIMENTATION ON THE TONGA FOREARC RELATED TO ARC RIFTING, SUBDUCTION EROSION, AND RIDGE COLLISION: A SYNTHESIS OF RESULTS FROM SITES 840 AND 841¹

Peter D. Clift,² Ulrich Bednarz,³ Reidulv Bøe,⁴ R. Guy Rothwell,⁵ Richard A. Hodkinson,⁶
Jaqueline K. Ledbetter,⁷ Cristelle E. Pratt,⁸ and Sione Soakai⁹

ABSTRACT

The sedimentary succession drilled at Sites 840 and 841 on the Tonga forearc allows the sedimentary evolution of the active margin to be reconstructed since shortly after the initiation of subduction during the mid Eocene. Sedimentation has been dominated by submarine fan deposits, principally volcanoclastic turbidites and mass-flows derived from the volcanic arc. Volcanoclastic sedimentation occurred against a background of pelagic nannofossil sedimentation. A number of upward-fining cycles are recognized and are correlated to regional tectonic events, such as the rifting of the Lau Basin at 5.6 Ma. Episodes of sedimentation dating from 16.0 and 10.0 Ma also correlate well with major falls in eustatic sea level and may be at least partially caused by the resulting enhanced erosion of the arc edifice. The early stages of rifting of the Lau Basin are marked by the formation of a brief hiatus at Site 840 (Horizon A), probably a result of the uplift of the Tonga Platform. Controversy exists as to the degree and timing of the uplift of Site 840 before Lau Basin rifting, with estimates ranging from 2500 to 300 m. Structural information favors a lower value. Breakup of the Tonga Arc during rifting resulted in deposition of dacite-dominated, volcanoclastic mass flows, probably reflecting a maximum in arc volcanism at this time. A pelagic interval at Site 840 suggests that no volcanic arc was present adjacent to the Tonga Platform from 5.0 to 3.0 Ma. This represents the time between separation of the Lau Ridge from the Tonga Platform and the start of activity on the Tofua Arc at 3.0 Ma. The sedimentary successions at both sites provide a record of the arc volcanism despite the reworked nature of the deposits. Probe analyses of volcanic glass grains from Site 840 indicate a consistent low-K tholeiite chemistry from 7.0 Ma to the present, possibly reflecting sediment sourcing from a single volcanic center over long periods of time. Trace and rare-earth-element (REE) analyses of basaltic glass grains indicate that thinning of the arc lithosphere had begun by 7.0 Ma and was the principle cause of a progressive depletion of the high-field-strength (HFSE), REE, and large-ion-lithophile (LILE) elements within the arc magmas before rifting. Magmatic underplating of the Tofua Arc has reversed this trend since that time. Increasing fluid flux from the subducting slab since basin rifting has caused a progressive enrichment in LILEs. Subduction erosion of the underside of the forearc lithosphere has caused continuous subsidence and tilting toward the trench since 37.0 Ma. Enhanced subsidence occurred during rifting of the South Fiji and Lau basins. Collision of the Louisville Ridge with the trench has caused no change in the nature of the sedimentation, but it may have been responsible for up to 300 m of uplift at Site 840.

INTRODUCTION

The Tonga forearc of the southwest Pacific Ocean represents a classic example of an intraoceanic forearc terrain. The Tonga arc system occurs along a nonaccretionary destructive plate margin where subduction has been continuous and west-dipping since its initiation in the mid Eocene (Hawkins et al., 1984). Ocean Drilling Program (ODP) Leg 135, by drilling the Tonga forearc basin, has provided an excellent opportunity to chart its sedimentary evolution and to relate this to tectonic and magmatic processes at the plate boundary. Two sites were drilled during Leg 135: one on the Tonga Platform (Site 840), and another on the upper trench slope (Site 841). Particular questions that were addressed by the drilling include the relationship

between backarc spreading in the Lau and South Fiji basins to forearc sedimentation, the role of subduction erosion/accretion in subsidence, and sedimentation, the provenance of the volcanoclastic sediments and their relationship to the arc volcanism, and the effect of eustatic sea-level changes on the sedimentary evolution.

Site 840 did not reach igneous basement; however, by attempting to reach a Miocene seismic discontinuity within the succession (Horizon A; Austin et al., 1989), results achieved at this site provide a detailed record of the last 7.0 m.y., including the critical pre- and syn-rift period of Lau Basin opening (Parson, Hawkins, Allan, et al., 1992). Site 841 allows the long-term sedimentary history of the forearc to be examined, as Hole 841B reached basement after penetrating a condensed section of late Eocene to present age. The goal of this paper is to summarize the principle features of the sedimentary sections drilled at Sites 840 and 841 and to comment on their implications for sedimentation in active margin environments, arc magmatic and chemical evolution during backarc basin formation, as well as changes in eustatic sea level.

Site 840 is located on the flank of the Tonga Platform (Fig. 1) approximately 45 km east-northeast of Ata Island. At this site the platform is about 60 km wide at the 1000 m isobath. The water depth is 743 m at Site 840, deepening to more than 10,000 m eastward (Tonga Trench) and to approximately 2,500 m westward (Lau Basin). Toward the west the general trend of increasing water depth is broken by the linear chain of seamounts and volcanoes of the Tofua Arc. Site 841 is located on the upper trench slope west of the axis of the Tonga Trench (Fig. 1) in a water depth of 4810 m. The site is 150 km east of the volcanic island of Ata and 235 km southeast from the uplifted coral platform of Tongatapu.

The forearc has been affected by almost continuous extensional deformation since the Eocene (MacLeod, this volume). In particular,

¹ Hawkins, J., Parson, L., Allan, J., et al., 1994. *Proc. ODP, Sci. Results* 135: Ocean Drilling Program (College Station, TX).

² Grant Institute, Department of Geology and Geophysics, The University of Edinburgh, West Mains Road, Edinburgh EH9 3JW, Scotland, United Kingdom (present address: Ocean Drilling Program, Texas A&M University, 1000 Discovery Drive, College Station, Texas 77845-9547, U.S.A.).

³ Forschungszentrum für Marine Geowissenschaften, Christian-Albrechts Universität, Postfach 102148, Wischofstrasse 1-3, D-2300 Kiel 14, Federal Republic of Germany (present address: Das Baugrund Institut, Brosshauser Str. 27, 5650 Solingen 11, Federal Republic of Germany).

⁴ Geological Survey of Norway, Trondheim, Norway.

⁵ Institute of Oceanographic Sciences, Deacon Laboratory, Brook Road, Wormley, Godalming, Surrey GU8 5UB, United Kingdom.

⁶ Department of Geology, Royal School of Mines, Imperial College, Prince Consort Road, London SW7 2BP, United Kingdom.

⁷ Department of Geosciences, University of Tulsa, 600 South College Avenue, Tulsa, OK 74104, U.S.A. (present address: Ocean Drilling Program, Texas A&M University, 1000 Discovery Drive, College Station, Texas 77845-9547, U.S.A.).

⁸ Mineral Resources Department, CCOP/SOPAC, Private Mail Bag, Suva, Fiji.

⁹ Ministry of Lands, Surveys, and Natural Resources, P.O. Box 5, Nukualofa, Tonga.

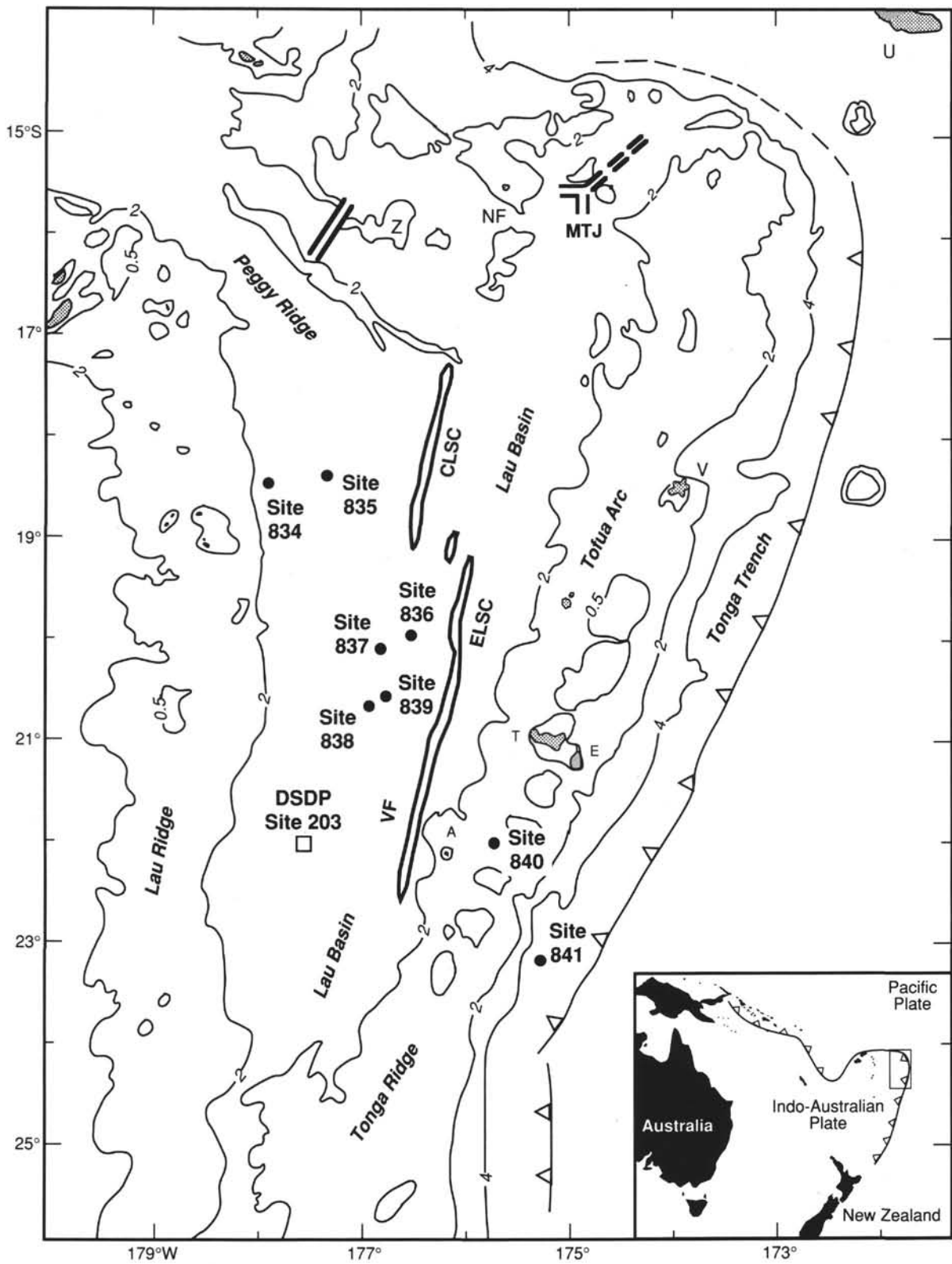


Figure 1. Map showing location of ODP sites drilled in the Lau backarc basin, western Pacific, during Leg 135. Also shown are the main geological features of the Tonga Trench and Lau Basin system. Islands shown are Tongatapu (T), 'Eau (E), 'Ata (A), Upolu (U), Vava'u (V), and Niufo'ou (NF). Locations of the Central Lau (CLSC) and East Lau (ELSC) spreading centers, Valu Fa Ridge (VF), and Mangatolu Triple Junction (MTJ) are also shown.

the volcanic arc has been rifted twice during formation of backarc basins: the South Fiji Basin (37.0–24.0 Ma; Weissel and Watts, 1975) and the Lau Basin (6.0–0.0 Ma; Parson, Hawkins, Allan, et al., 1992). In each case, the forearc was separated from its volcanic arc, which then formed a remnant arc before volcanic activity recommenced on a new volcanic arc on the trench side of the basin. Thus, before the initiation of rifting and backarc seafloor spreading in the Lau Basin, the Lau and Tonga Ridges would have formed a single magmatic arc/forearc succession (Packham, 1978; Hawkins et al., 1984). The two sites drilled during Leg 135 allow comparisons to be made across the forearc and provide the opportunity to examine the rift and immediate pre-rift history at Site 840, whereas the more condensed section at Site 841 records the late Eocene–early Miocene history not reached at Site 840. Apart from the shallow-water carbonates of late Eocene–early Oligocene age at Site 841, sedimentation has been characterized by a pelagic, usually carbonate, background component with variable amounts of volcanoclastic input. Throughout the Miocene, discontinuous deposition of volcanoclastic sediment and associated pelagic/hemipelagic sediments occurred in the forearc region of the Lau Ridge (Scholl et al., 1985; Herzer and Exxon, 1985). After 5.0 Ma, the Tonga Platform (Site 840) evolved into a gently subsiding, shallow-marine carbonate platform, whereas the upper trench slope at Site 841 continued subsidence and sediment starvation.

THE SEDIMENTARY SEQUENCES

Sedimentology

Site 840

The sedimentary sequence recovered at Site 840 is 597.30 m thick and is divided into three lithostratigraphic subunits (Fig. 2A; see Parson, Hawkins, Allan, et al., 1992, pp. 500–520). Unit I (0–109.98 mbsf; upper Pliocene to upper Pleistocene) consists of clayey nannofossil oozes and vitric nannofossil oozes with clay. Vitric silts and sands, pumiceous gravels, and pyroclastic deposits occur in subordinate amounts. The dominant lithology in the upper part of Unit I is soft, homogeneous, pelagic, white to light brownish gray, clayey nannofossil ooze. Bioturbation is pervasive in the lower part of the unit but decreases upward. The carbonate content of the pelagic sediments ranges from 50% to 86%. Foraminifers are generally well preserved and abundant, and bioclasts include shell fragments and echinoderm spines.

The lithostratigraphic boundary between Units I and II is marked by a sharp downward transition at 109.98 mbsf from structureless nannofossil ooze to indurated highly bioturbated pelagic and hemipelagic marl. Unit II (109.98–260.50 mbsf; upper Pliocene to upper Miocene) contains three depositional cycles fining upward from predominantly un lithified pumiceous gravels into predominantly indurated nannofos-

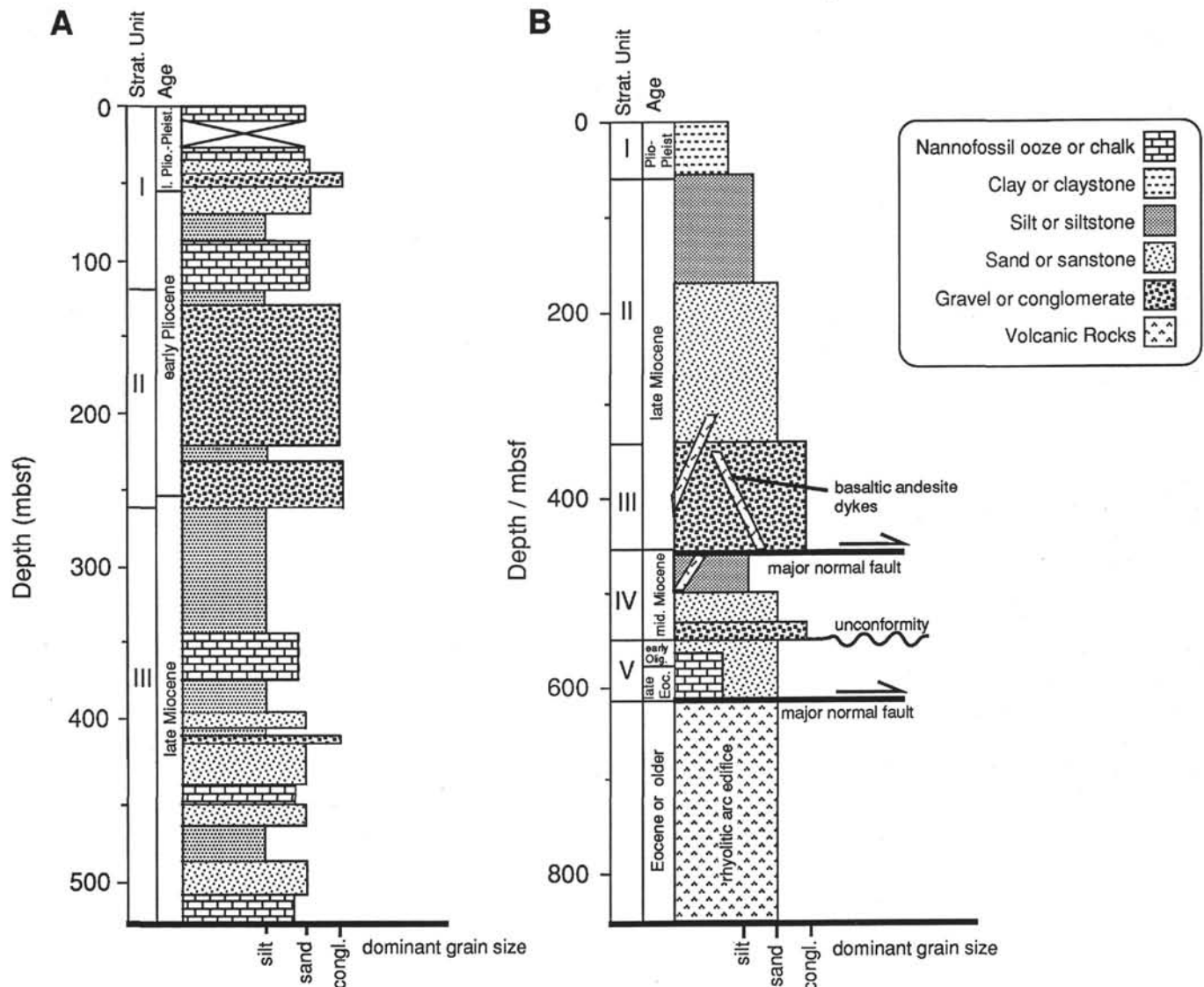


Figure 2. Simplified sedimentary log of the section at Sites 840 (A) and 841 (B). Logs derived from recovered core and associated FMS imaging (Clift, this volume).

sil chalk. Volcaniclastic sediments typically consist of vitric sand and sandstone with sharp sporadically scoured basal contacts. This lithology fines upward into vitric silt or siltstone. The upper contact of the volcaniclastic sediments with the pelagic marl or marlstone is usually obscured by pervasive bioturbation. The CaCO₃ content of the marls and marlstones ranges from 53% to 41%, with a decreasing content downhole. Carbonate bioclasts are absent in Unit II, and foraminifers are poorly preserved and decrease in abundance downhole.

Unit III (260.5–597.3 mbsf; upper Miocene) consists of an indurated sequence of vitric and volcanic siltstone and sandstone turbidites, interbedded with highly bioturbated silty marlstones. The transition from Unit II to Unit III is marked by a rapid fining of the section from a sequence dominated by coarse volcanic sands and gravels above 260.5 mbsf to one dominated by pelagic chalks and volcaniclastic silt below. In the lower part of the unit, beds of volcanic breccia and volcanic conglomerate also occur. A majority of the turbidites show sharp, planar basal surfaces, but undulating, scoured basal surfaces. Surfaces with load casts are also common. Downhole through Unit III, individual turbidites show an increase in thickness and both the average and the maximum grain size of clasts in the turbidites increases. The pelagic intervals show no systematic variation in bed thickness vs. depth; however, the carbonate content decreases from a maximum of 50% near the top of the unit to a low of 24% near the base as clay becomes an increasingly dominant constituent of these pelagic intervals.

Site 841

The sedimentary succession recovered at Site 841 is 605 m thick and is divided into five lithostratigraphic subunits (Fig. 2B; see Parson, Hawkins, Allan, et al., 1992, pp. 585–598). Unit I (0–56.0 mbsf; middle Pleistocene–Pliocene) is composed of a sequence of structureless clays, with thin- to medium-bedded turbidites of vitric sand and vitric silt, as well as primary air-fall ash deposits. Below 17.5 mbsf, nannofossils disappear from the sediments, and the resulting clay appears homogeneous over long intervals. At its lower boundary, Unit I passes down gradationally from volcanic clay into a volcanic silty gravel and siltstone sequence.

The uppermost part of Unit II (56.0–333.2 mbsf; Pliocene–upper Miocene) is composed of silty gravel and vitric silt, which passes downward into clay with glass, vitric clay, vitric silt, vitric sand, and thin pyroclastic deposits. Below 81.4 mbsf, the sequence consists of clay, vitric siltstone, clayey siltstone, and vitric sandstone; below 169.8 mbsf the sediments are vitric siltstones and vitric sandstones. Moving downsection, the proportion of sandstone, as well as bed thickness and grain size, increases. These deposits show a wide variety of sedimentary structures (Parson, Hawkins, Allan, et al., 1992, pp. 589–590).

Unit III (332.2–458.1 mbsf; upper Miocene) is composed of volcanic conglomerate and breccia, vitric sandstone, and vitric siltstone. The upper part of the unit above 385.0 mbsf shows an upward-fining trend. Indeed, the transition downward from Unit II is one characterized by the appearance of volcanic conglomerate interbedded with the volcanic siltstones and sandstones below the contact. A basaltic dike occurs in the middle of the unit, and in the lower part of the unit there is a fault breccia. Microfaulting is also observed throughout the unit. The lower boundary of Unit III is a major fault.

Unit IV (458.1–549.1 mbsf; lower middle Miocene) consists of volcanic siltstones and sandstones, but below 535.0 mbsf volcanic conglomerates and breccias also occur. The deposits are organized in an overall upward-fining sequence. Tectonic and soft-sediment deformation occur throughout the unit, and the sediments show a reticulate pattern probably caused by hydrothermal fluid circulation and leaching. The lower boundary of Unit IV is an unconformity spanning approximately 13 m.y. The boundary is faulted and consists of a fault breccia.

The upper part of Unit V (549.1–605.0 mbsf; lower Oligocene–upper Eocene) is composed of clayey, calcareous, volcanic sandstone with foraminifers, with beds of volcanic conglomerate, sandy clay-

stone, clayey sandstone, and claystone. Below this lies calcareous volcanic sandstones, and in the lower part of the unit the dominant lithologies are calcareous volcanic sandstones with large foraminifers and large foraminifer bioclastic volcanic sandstone. At the base of Unit V there is a faulted contact with a rhyolitic volcanic complex.

Environment of Deposition

Site 840

The volcaniclastic sediments of Unit III at Site 840 were deposited as turbidites. Numerous examples of complete Bouma sequences (Bouma, 1962) occur. The majority of these were probably deposited from low-concentration flows (e.g., Stow and Shanmugan, 1980; Bøe, this volume). In the lower part of the unit, traction carpet deposits and turbidites possibly deposited from high-concentration turbulent flows are also present (e.g., Einsele, 1991; Bøe, this volume).

The predominance in the lower part of Unit III of relatively thick and coarse-grained turbidites with abundant convoluted bedding indicates deposition from large flows in a setting not far from the source area (Bøe, this volume). Thinning and fining of turbidites upward through Unit III probably resulted from reduced sediment supply because of waning volcanic activity in the source area. The petrology of the volcaniclastic grains and the phase chemistry of glass indicates a decreasing supply of volcaniclastic material from a source of consistent tholeiitic character possibly a single seamount or a volcanic island (Bøe, this volume; see below). Unit III was probably deposited as a submarine sheet fan system with sediment transport eastward from the forearc.

The boundary between Units III and II reflects a change back to more coarse-grained and rapid deposition. The sediments of Unit II are dominated by thick-bedded pumiceous gravels and sands interpreted as sediment gravity-flow deposits, predominantly turbidites but debris-flow deposits may also occur. Close proximity to the volcanic source is suggested by the large volumes of rhyodacitic pumice deposited within only 1.5 m.y. In the uppermost 10–15 m of Unit II, the sedimentary sequence is dominated by nannofossil chalks, implying a decrease in the rate of volcaniclastic sediment supply.

The lower part of Unit I, below 95.0 mbsf, is dominated by nannofossil chalks slowly deposited with minimal terrigenous or volcaniclastic input. At 95 mbsf, a 1-m.y. biostratigraphic hiatus marks the boundary toward slowly deposited hemipelagic nannofossil oozes interbedded with thin volcaniclastic turbidites. In the uppermost part of the unit, thin pyroclastic fallout tephra occur.

Site 841

The first sediments deposited at Site 841 were the products of rhyolitic, subaerial volcanism and were deposited as pyroclastic air-fall tuffs. At the upper boundary of Unit V, a change occurs in the sedimentary sequence that was deposited in a shallow-water marine carbonate environment. The sequence shows evidence of episodic emplacement of volcanic sand from a nearby volcanic center (Parson, Hawkins, Allan, et al., 1992, pp. 594–595) in the form of two major upward-fining cycles Units III to I and Unit IV.

The sedimentary hiatus between the early Oligocene and the early/middle Miocene (boundary between Units V and IV) marks a change toward an upward-fining sequence of volcaniclastic turbidites. Volcaniclastic sediments in the lower part of the upper Miocene (Unit II) again comprise volcanic sandstones and conglomerates deposited as turbidites and other sediment gravity-flow deposits. These sediments accumulated rapidly, based on the high density turbidite facies and the biostratigraphy (Parson, Hawkins, Allan, et al., 1992, pp. 602–614), probably in a proximal position relative to the source area. Upward, there is a transition into thin- to medium-bedded sands and silts (Unit II) and finally into clayey siltstones with thin sandstones interpreted as distal turbidites. From the late Miocene to the middle Pleistocene, hemipelagic clays with minor interbedded volcaniclastic tur-

bidites and thin pyroclastic ash layers were deposited (Unit I; Parson, Hawkins, Allan, et al., 1992, pp. 585–589).

SUBSIDENCE HISTORY

Sediments recovered at Sites 840 and 841 record the complex interplay of tectonics and eustasy in controlling the sedimentation in active plate margin settings. Sediment backstripping techniques (e.g., Sclater and Christie, 1980) can be used in conjunction with traditional facies analyses to reconstruct the sedimentary and subsidence history of the Tonga forearc. Critical in this approach is the accurate dating of the recovered sections and determination of the paleowater depth in which the sediments were deposited.

Estimates of water depth were made using the composition of the microfaunal assemblages their state of preservation (Parson, Hawkins, Allan, et al., 1992, pp. 523–526 and 602–614), and any associated trace fossils (e.g., Ekdale, Bromley, and Pemberton, 1984) produced by macrofauna not preserved in the core. Clift (this volume) detailed paleowater depth estimates at each site (Table 1). However, there are two opposing paleowater depth interpretations for Site 840 (see the following).

According to Clift (this volume), the sedimentary and paleontological data at Site 840 suggest that the water depth has remained at approximately the modern value throughout the section cored. This interpretation is based on the pelagic and benthic microfauna assemblage, the general lack of calcite dissolution (restricting deposition to being above the lysocline), and the presence of the trace fossil *Thalassinoides* sp. within the *Zoophycos* ichnofacies. Although *Thalassinoides* sp. is known to exist as deep as 3000 m (Hayward, 1976), this is rare and it is generally found in abundance in water depths of less than 600 m. These features are interpreted by Clift (this volume) as indicating deposition within a depth range of approximately 300 to 600 m. Seismic data (Austin et al., 1989) and structural information from cores point to subsidence of the platform in its present paleogeographic state by the progressive rotation of the Tonga Platform at Site 840 and rule out dramatic uplift or subsidence events (Clift, this volume).

Ledbetter and Haggerty (this volume) suggested a different interpretation. Bioturbation is an ubiquitous feature of the pelagic intervals

in the cores recovered from Site 840, particularly in Units II and III. According to Ledbetter and Haggerty, discrete bioturbated intervals are comparable to the bathyal and abyssal assemblages described by Berger et al. (1979) and Ekdale, Muller, and Novak (1984). *Planolites* and *Thalassinoides* burrows show a slight but regular increase in diameter upcore suggestive of increasing bottom-water oxygenation. The diameter of the burrows with spreiten show more scatter but decrease slightly with time. This is interpreted as implying an increase in bottom-water oxygenation and a corresponding increase in the rate of oxidation of organic matter in the sediments going upsection in the upper Miocene (Unit III). Ledbetter and Haggerty considered the upward increase in bottom water oxygenation to be the result of rapid, tectonically driven shoaling caused by Lau Basin rifting, effectively comparable to rift-flank uplift seen in continental rift settings (e.g., Keen, 1985).

The carbonate content of the pelagic and hemipelagic sediments below 120.0 mbsf is uniformly low, and the abundance of foraminifers decreases downward. Foraminifer preservation is generally poorer within burrows filled with pelagic sediment derived from the seafloor than in the redeposited volcanoclastic host sediment (Ledbetter and Haggerty, this volume). The low abundance and poor preservation of foraminifers observed in pelagic sediments below 120.0 mbsf is interpreted by Ledbetter and Haggerty as a result of dissolution. Foraminifers in redeposited sediments are better preserved because they are protected from this dissolution by rapid downslope transport followed by rapid burial. The foraminifer lysocline during the late Miocene was probably at about 2800 m (van Andel, 1975). This is interpreted as suggesting that all of the sediments of Unit III were deposited at or near this depth (Ledbetter and Haggerty, this volume). This dissolution is seen to finish within Unit II. A conservative estimate of the paleowater depth would be somewhere between 2000 and 2500 m. The better preservation and higher abundance of foraminifers above 120.0 mbsf suggest water depths similar to those found on the Tonga Platform today (Ledbetter and Haggerty, this volume). This alternative scenario involves a rapid uplift of around 2000 m of Site 840 during the upper Miocene–early Pliocene (i.e., during the rifting of the Lau Basin). Clift (this volume) contested that such large uplift is difficult to reconcile

Table 1. Sedimentary thicknesses, lithologies, ages, and interpreted paleowater depths for Sites 840 and 841.

| Depth to base of interval (m) | Depth to top of interval (m) | Age at base (Ma) | Age at top (Ma) | Paleowater depth (m) | Lithology | CCD | Lysocline |
|-------------------------------|------------------------------|------------------|-----------------|----------------------|------------------------|------|-----------|
| Site 840: | | | | | | | |
| 752.5 | 743.0 | 0.50 | 0.40 | 740 | Chalk | 4400 | 3900 |
| 771.4 | 752.5 | 1.80 | 1.70 | 300–600 | Chalk | 4300 | 3800 |
| 780.9 | 771.4 | 1.90 | 1.80 | 300–600 | Chalk | 4300 | 3800 |
| 800.0 | 780.9 | 2.65 | 1.90 | 300–600 | Sandstone | 4200 | 3700 |
| 819.0 | 800.0 | 3.00 | 2.65 | 300–600 | Sandstone | 4200 | 3700 |
| 838.7 | 819.4 | 3.50 | 3.10 | 300–600 | Chalk | 4100 | 3600 |
| 848.4 | 838.7 | 4.90 | 4.50 | 300–600 | Chalk | 4100 | 3600 |
| 935.0 | 848.4 | 5.20 | 4.90 | 300–600 | Conglomerate/sandstone | 4000 | 3500 |
| 1002.7 | 935.0 | 5.25 | 5.20 | 300–600 | Conglomerate/sandstone | 4000 | 3500 |
| 1031.8 | 1002.7 | 5.30 | 5.25 | 300–600 | Sandstone | 4000 | 3500 |
| 1041.5 | 1031.8 | 5.60 | 5.30 | 300–600 | Chalk | 4000 | 3500 |
| 1070.5 | 1041.5 | 5.80 | 5.60 | 300–600 | Siltstone | 4000 | 3500 |
| 1166.9 | 1070.5 | 6.50 | 5.80 | 300–600 | Siltstone/chalk | 4000 | 3500 |
| 1340.3 | 1166.9 | 7.10 | 6.50 | 300–600 | Sandstone | 4000 | 3500 |
| Site 841: | | | | | | | |
| 5426.0 | 5413.9 | 37.50 | 37.30 | 0–100 | Chalk | 3400 | 2900 |
| 5413.9 | 5370.1 | 37.30 | 35.50 | 100–2700 | Sandstone | 3200 | 2700 |
| 5370.1 | 5366.0 | 35.50 | 35.00 | 2700–3200 | Sandstone | 3700 | 3200 |
| 5366.0 | 5269.5 | 16.20 | 14.90 | 100–3800 | Sandstone | 4300 | 3800 |
| 5269.5 | 5096.6 | 10.00 | 9.00 | 3900–4200 | Sandstone | 3900 | 3400 |
| 5096.6 | 4886.5 | 9.00 | 5.30 | 4200–4500 | Sandstone | 4200 | 3700 |
| 4886.5 | 4821.0 | 5.30 | 0.00 | 4800 | Shale | 4300 | 3800 |

Notes: Interpreted paleowater depths according to the model of Clift (this volume). Two models have been set forth for Site 840 (see discussion in text), the first (Model A; Clift, this volume, tabled here) proposing consistent moderate depths, and the second (Model B; Ledbetter and Haggerty, this volume) indicating greater water depths during the Miocene.

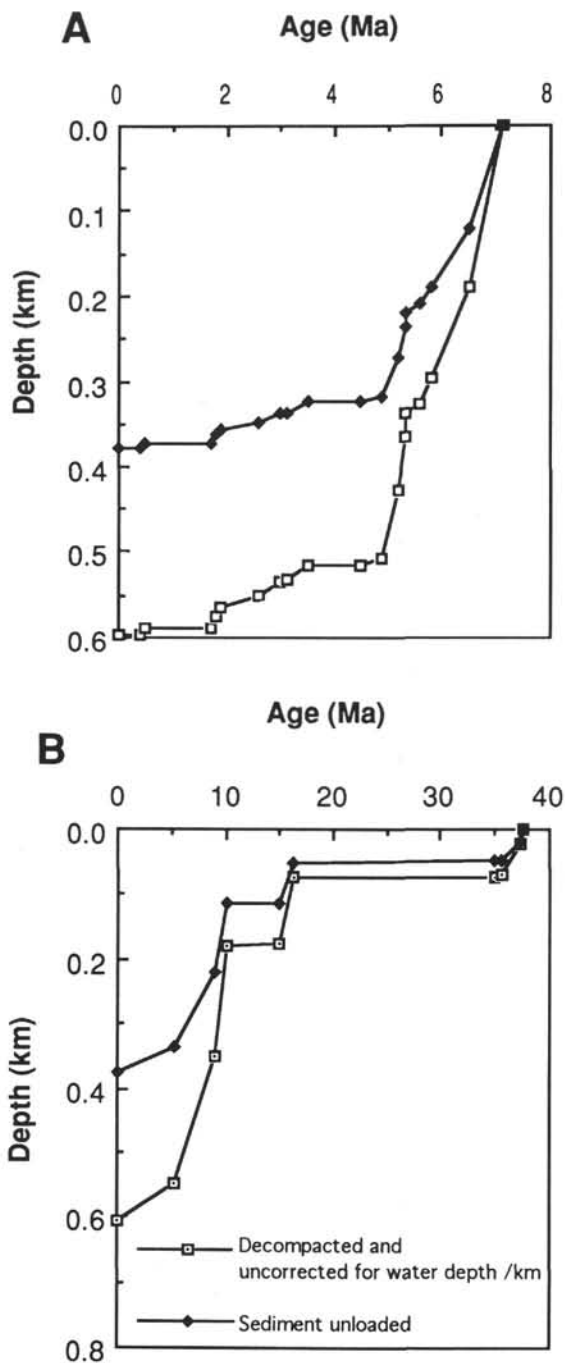


Figure 3. Decompacted and water-unloaded subsidence curves calculated for the sedimentary section drilled at Sites 840 (A) and 841 (B), showing the subsidence of the basement relative to present sea level. No correction for paleowater depth is made.

with the modest post-rift subsidence, as well as the seismic stratigraphy of the Tonga Platform (Austin et al., 1989).

The sedimentary section at Site 841, which presently lies at 4850 m, spans a much longer time period, representing 37.0 m.y. Water-depth determinations are difficult at such extreme depths. Nevertheless, the presence of shallow-water foraminifers *Discocyclina* sp. at the base of the section provides a precise water depth within the photic zone at 37.0 Ma (Parson, Hawkins, Allan, et al., 1992, p. 614). However, by 35.0 Ma the corrosion of nannofossils and the disappearance

of benthic foraminifers indicates that Site 841 had subsided below the lysocline. Although water depth estimates for the time between 35.0 and 16.2 Ma cannot be made because of a sedimentary hiatus during this time period, the excellent preservation of nannofossils above the unconformity indicates that water depths were then above the lysocline. Exactly whether this implies an uplift of Site 841 during the period of the hiatus or not is debatable because van Andel (1975) showed that the depth of the carbonate compensation depth (CCD) and lysocline had deepened significantly in the Pacific between the early Oligocene and the middle Miocene. Structural information (MacLeod, this volume, chapter 20) shows a gradual tilting of Site 841 toward the trench since the start of sedimentation. Although not conclusive, this fact argues against any dramatic uplift and favors either a small amount of uplift or even some subsidence over the period of the hiatus. Further water deepening is demonstrated by a subsequent appearance of corroded nannofossils, and thus deposition close to the CCD (3900 m) by 10.0 Ma, and eventually their final disappearance as Site 841 passes through the CCD (4200 m) at 5.3 Ma.

Using the water-depth estimates of Clift (this volume), and the age and lithologic information (Table 1), the subsidence history of the two sites has been calculated using the backstripping technique of Sclater and Christie (1980). This reconstruction assumes that the crust behaves according to Airy isostasy, a condition most likely to be met if the forearc has been in extension throughout the period concerned. The presence of normal faults throughout the core at Sites 841 and 840 suggests that this has been the case, except during the collision of the Louisville Ridge with the section of the Tonga Trench directly opposite Site 841 at approximately 2.0 Ma (Dupont and Herzer, 1985). Because this would affect only a small section of the reconstruction at Site 841, and does not seem to have any effect within the errors of the water depth estimate at Site 840 (Clift, this volume), the isostatic criterion can be met. Additional compaction of the sediment, above that calculated by Sclater and Christie (1980) for shallow-water depths, owing to the large water load at Site 841 is thought to be negligible.

Figure 3 shows the calculated subsidence for the basement at both Sites 840 and 841 (Clift, this volume). The two curves shown are corrected, first, for compaction only and, second, for compaction and sediment loading. No attempt has been made to correct for paleowater depth. As such, these diagrams reflect accumulation rates rather than subsidence rates. Figure 3 shows rapid deposition at Site 840 up to 5.3 Ma, after which deposition increased for a short time but subsequently slowed down to a relatively modest rate after 4.9 Ma. In contrast, Site 841 shows three depositional episodes. Modest rates of sedimentation operated between 37.0 and 35.0 Ma. Sedimentation was probably continuous from 35.0 Ma until almost 16.2 Ma, when erosion may have removed large amounts of the section, leaving a fining-upward cycle dating from 16.2 to 14.0 Ma. Similarly, sedimentation is assumed to have continued between 14.0 and 10.0 Ma, a period removed by more recent normal faulting. The upward-fining cycle dating from 10.0 Ma may thus have been initiated before this time.

Figure 4 shows the sections at each site corrected for variations in paleowater depth, as well as the corrections applied in Figure 3 (Clift, this volume). The two curves for each site correspond to minimum and maximum depth estimates. At Site 840, the minimum and maximum depths (assuming paleowater depths of 300–600 m) show parallel trends similar in form to the uncorrected version, reflecting the way that subsidence at Site 840 has been balanced by sedimentation. The period up to 5.3 Ma shows rapid basement subsidence, which increases again after 5.3 Ma and subsequently slows to a gradual decline from 4.9 Ma to the present. The apparent rapid subsidence between 1.69 Ma and the present is purely the result of a poor water-depth estimate at 1.69 Ma because no major deepening is inferred for this time period on the basis of the sedimentary evidence (Clift, this volume). Site 841, however, shows significant differences between the calculated minimum and maximum paleowater depths. Although both curves predict a major basement subsidence event at 35.5 Ma, a significant discrep-

ancy is present between the two models from 35.0 Ma to the present. The maximum water depth shows a steady subsidence since 35.0 Ma, whereas the minimum estimate predicts some basement uplift between 35.0 and 16.2 Ma, and subsequent strong subsidence at 16.2 Ma. As mentioned previously, structural data (MacLeod, this volume) suggest a gradual tilting and subsidence of Site 841, thus favoring the maximum water-depth estimate.

The result of the subsidence analyses (Clift, this volume) at Sites 840 and 841 suggests that subsidence of the Tonga forearc has been a continuous process since early in the subduction history. Subsidence is seen to peak at 5.3 and 35.5 Ma, with a possible third event at 16.2 Ma. Interestingly, the events at 5.3 and 35.5 Ma correlate well with arc-rifting episodes in the active margin, before the formation of the Lau and South Fiji backarc basins, respectively (Parson, Hawkins, Allan, et al., 1992; Weissel and Watts, 1975). If subsidence is present at 16.2 Ma, this does not seem to correlate well with any known tectonic event in the region. Instead, this event may be controlled by extensional faulting in the forearc, owing to the ongoing subduction erosion of the plate margin. If a major fault was initiated close to Site 841 at 16.2 Ma, then this might explain the influx of coarse clastic material as well as any deepening that may have occurred.

Although the influx of coarse clastic material at 10.0 Ma does not seem to translate into tectonically driven subsidence when water depths are accounted for, this may reflect the difficulty in making an accurate water-depth estimate at such depths. One reason for thinking that the forearc may experience a boost in tectonic subsidence at that time comes from the rapid subsidence noted at Site 840 that was already underway at 7.1 Ma (Clift, this volume). According to Clift, the shallow water depths at this site provide much firmer evidence for subsidence dating from at least 7.1 Ma and conceivably starting at 10.0 Ma. Exactly what the cause of this tectonic subsidence would be is unclear. One possible candidate could be the extension and rotation of the Tonga Arc following the reversal of subduction polarity in the New Hebrides section of the plate boundary (Moberly, 1971).

The Role of Eustasy

As discussed previously, there are good reasons to think that tectonics is the single most important factor governing sedimentation on the Tonga forearc. Nevertheless, predicted large-magnitude falls in eustatic sea level (Haq et al., 1987), which might be expected to accentuate erosion of the arc edifice, correlate well with influxes of sediment at Site 841 (Clift, this volume). Although enhanced tectonic subsidence may have started at 16.2 Ma and caused deposition of a fining-upward cycle from 16.2 to 10.0 Ma, it is noteworthy that this same period is marked by a long-term, large-magnitude fall (approximately 80 m; Haq et al., 1987) in eustatic sea level, which could equally have been the cause of this sediment influx. Similarly, the influx of sediment at 10.0 Ma at Site 841 correlates well with a major fall (approximately 150 m) in sea level at this time.

The large number of sea-level fluctuations close to 5.3 Ma may suggest that the peak in sedimentation at Site 840 at this time may also be controlled by sea level. However, with so many proposed sea-level falls in this time period, it is difficult not to correlate a sedimentary event with a fall. Importantly, if sea-level fall is responsible for the pulse of sedimentation seen at Site 840 at 5.3 Ma, then the absence of similar sequences coinciding with other subsequent falls in sea level of similar magnitude is problematic. In conclusion, it seems probable that sea level has played some part in controlling sedimentation in the forearc, principally in accentuating the effect of tectonic subsidence. Large-scale, long-term (1–5 m.y.) variations in sea level seem to be more obvious than the short-term variations. Fining-upward cycles dating from 16.2 and 10.0 Ma at Site 841 are the most likely candidates for being principally controlled by eustasy, because of their good correlation with the Haq et al. (1987) curve, and the difficulty in correlating them with regional tectonic events at times that might otherwise have triggered the sedimentation observed.

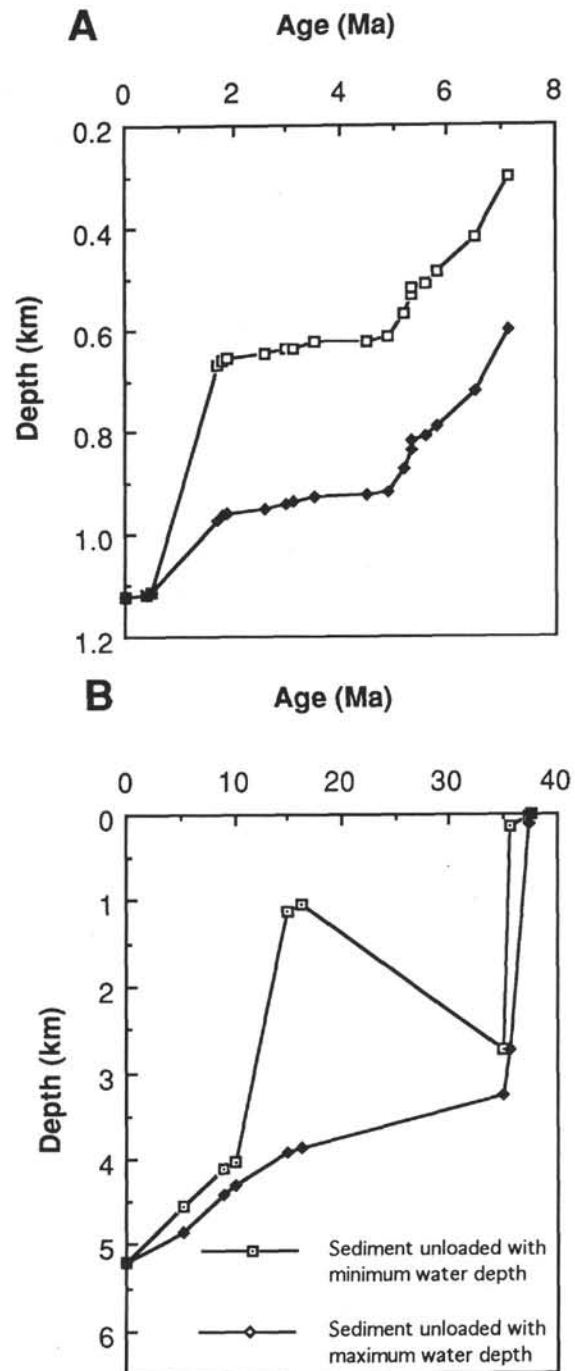


Figure 4. Decompacted and water-unloaded subsidence curves with correction for paleowater depths (values of Clift, this volume) at Sites 840 (A) and 841 (B).

Tectonics and Sedimentation

Site 840 is situated in a heavily faulted region, and the sedimentary sequence reflects the different tectonic events that occurred during the history of deposition. Below approximately 500 mbsf (approximately 6.1 Ma), a sudden increase takes place in the bedding dip. This change is accompanied by changes in physical properties, grain size, clay content, and microfossil abundance (Bøe, this volume; Ledbetter and Haggerty, this volume) and can probably be explained by faulting, with westward tilting of the block on which Site 840 is situated.

Between 500 and 260 mbsf (Parson, Hawkins, Allan, et al., 1992), the bedding dip steadily decreases, which probably results from

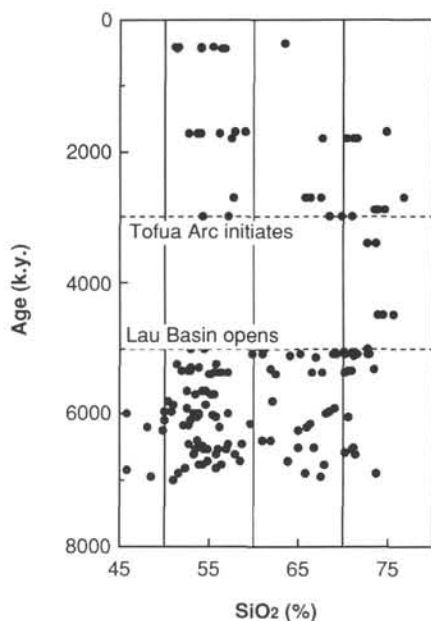


Figure 5. Diagram showing the variation in total silica contents of volcanic glass grains with age for Site 840 (Tonga Platform).

progressive syndepositional tilting of the block on which Site 840 is situated. At 383.0 mbsf (approximately 5.5 Ma), a change takes place in physical properties, carbonate content, grain size, and mean silica content of the volcanic sediment. A zone of strong sediment alteration also occurs. This break may mark the onset of rifting in the Lau Basin (Bøe, this volume). The age of the break corresponds closely with the age of the oldest known sediments in the Lau Basin, which are approximately 5.6 m.y. old (Parson, Hawkins, Allan, et al., 1992).

Horizon A, which has been interpreted as a regional, angular, seismostratigraphic unconformity (Herzer and Exon, 1985; Scholl et al., 1985), may correspond to the break in sonic velocity and density at about 383.0 mbsf (Bøe, this volume) or, possibly, to a similar break at about 500.0 mbsf (Ledbetter and Haggerty, this volume). Westward thickening of the succession above Horizon A, as seen on seismic-reflection profiles, occurs in conjunction with eastward onlapping against the structurally and geomorphologically higher Pacific side of the platform (Austin et al., 1989). This indicates post-Horizon A subsidence toward the Lau Basin, with the main source region for the sediments located to the west. A sudden decrease in grain size above 383.0 mbsf may be ascribed to a shift of the locus of coarse-grained deposition toward the west (Bøe, this volume). This occurred because of the extension and subsidence of the Tonga Arc during early rifting, curtailing the explosive, subaerial, volcanic eruptions that had previously formed the principle sediment source to the forearc platform (Clift and Dixon, this volume).

Before 5.6 Ma, during the initial rifting of the Lau-Tonga Ridge, sediments accumulated rapidly at Site 840. The sedimentary succession deposited between 5.6 and 5.3 Ma reflects a quieter period, with rifting and subsidence of the Lau-Tonga Ridge and without extensive volcanism (Bøe, this volume). In the period 5.3–5.25 Ma, sedimentation rates increased rapidly; and, at the boundary between Units III and II, at approximately 5.25 Ma, a change to much more coarse-grained and rapid deposition took place. This is interpreted as reflecting the onset of extensive rifting and volcanism in the proto-Lau Basin. Renewed progradation of large volumes of sediments into the forearc basin occurred because of a large supply of volcanic material in the source area (Bøe, this volume; Tappin et al., this volume). Similar influxes of rhyolite- and dacite-dominated material are known from other rifting backarc basin systems, such as the Sumisu Rift of the Bonin Arc (e.g., Nishimura et al., 1991; Taylor, 1992).

At approximately 5.1 Ma, near the top of Unit II, Dupont and Herzer (1985) and Ledbetter and Haggerty (this volume) interpreted the sedimentary sequence to reflect rapid uplift of the forearc and a widespread planation. This was then followed by local intense erosion. Uplift of the outer forearc may possibly have been a response to thermal upwelling related to the opening of the Lau Basin. In this case, the sedimentary hiatus near the base of Unit I (between 95.0 and 101.0 mbsf) probably resulted from the uplift of the forearc and may be ascribed to a period of nondeposition or erosion.

Alternatively, Clift (this volume) indicated exclusively rapid base-subsidence after 5.25 Ma, during final breakup of the forearc/arc system. In this case, uplift would be restricted to the earlier pre-breakup stage (i.e. the hiatus at 383.0 mbsf). Clift did not assign any importance to Horizon A at 383.0 mbsf because no uplift is shown at Site 840 by the reconstructed subsidence curves. However, other lines of evidence and regional considerations suggest that this break is significant as a pre-rift uplift unconformity. Importantly, within the subsidence estimates, some motion between the minimum and maximum water-depth estimates can be accounted for at this time (<300 m). Paleowater depth indicators are not accurate enough to constrain the uplift or subsidence at Site 841 because of the great water depth. The sedimentary hiatus between 95.0 and 101.0 mbsf is principally the result of the hiatus in arc volcanism on the trench side of the Lau Basin between 5.0 and 3.0 Ma, before foundation of the new Tofua Arc. Thermal heating of the forearc lithosphere would not have been a significant factor, as the lithosphere would have been heated before rifting by the volcanic arc itself, and in any case might be expected to have affected the Lau Basin side of the Tonga Platform more than the trench side, the opposite of what is observed. Following the final breakup of the Lau-Tonga Ridge after approximately 5.25 Ma, the Tonga Ridge developed into a carbonate platform with low sediment-accumulation rates, at approximately 4.9 Ma.

VOLCANICLASTIC EVOLUTION

The Tonga Platform was adjacent to an active volcanic arc throughout its history and provides a stratigraphic record of the adjacent arc volcanism. The sediments recovered at Site 840 have been used to reconstruct the volcanic evolution of the original Tonga Arc and modern Tofua Arc.

The sedimentary rocks at Site 840 consist of volcaniclastic debris and pelagic/hemipelagic components, the relative proportions of which vary systematically throughout the succession. Diagenesis has also resulted in some alteration and mineralization of the original sediments and varies in intensity both vertically in the section and from lithology to lithology. The volcaniclastic debris is immature and dominated by angular and broken glass shards, pumice clasts, igneous minerals, and rock fragments (Bøe, this volume).

Within Unit III, the SiO₂ content of volcanic glass ranges from 47% to more than 75%, covering the compositional range from basalt to rhyolite (Bøe, this volume; Clift and Dixon, this volume). Bøe used electron microprobe techniques to record a decrease in the silica content upsection, with an additional increase in silica content at about 400.0 mbsf. In contrast, Clift and Dixon (this volume) did not find any change in the range of silica values within Unit III (Fig. 5), but instead showed a complete spectrum of compositions. Plagioclase feldspars within Unit III show a range of compositions extending from An₉₅ to An₄₈. The majority of the feldspars are bytownite in composition (Bøe, this volume). The composition of plagioclase and volcanic glasses indicates derivation from volcanic rocks of low-K tholeiitic composition. Although a small number of analyses appear to fall in the calc-alkaline field, this may reflect mobilization of alkali elements during diagenesis. No alkaline pyroxene compositions are known from any part of Site 840 that may support the suggestion of calc-alkaline volcanism at this time, or at any other time (Clift and Dixon, this volume; Cawood, 1991). The trend to decreasing silica identified by Bøe (this volume) was ascribed to eruption from a fractionated magma chamber.

Indeed, the coherent tholeiitic trend may indicate derivation from a single volcanic source. This source must have been part of the original Tonga Arc, situated to the northwest of Site 840. As such, it is now preserved within the Lau Ridge or as rifted fault blocks within the western Lau Basin (Bøe, this volume).

Unit II at Site 840 is dominated by large volumes of rhyolitic to rhyodacitic pumice (approximately 70 wt% SiO₂), although again Clift and Dixon (this volume) did not record any change in the total range of the tholeiitic glasses. The coarse-grained nature of the gravels suggests close proximity to the volcanic source, which must have been either the Lau Ridge or a volcanic island within the proto-Lau Basin, as the only active volcanic features in the area. Very little volcanic material of any sort is present in the lower half of Unit I; however, the pyroclastic deposits in the upper part of Unit I are interpreted as proximal fallout tephra derived from the subaerial Tofua Arc, probably Ata Island. Although they occupy a similar range of silica contents as the glasses in Units II and III, these Unit I glasses were recorded by Clift and Dixon (this volume) as being principally of bimodal character (i.e., dacitic and basaltic andesite). In this respect, these youngest volcanic glasses are more like the glasses of the Lau Basin sediments (Bednarz and Schmincke, this volume; Clift and Dixon, this volume) than the glasses of Units II and III.

The transition at Site 840 from a volcanoclastic-dominated sequence in the Miocene/early Pliocene (Units II and III) to a carbonate-dominated sequence in the Pliocene-Pleistocene (Unit I) supports the idea that volcanism on the arc underwent a hiatus immediately after rifting. The relatively small size of the modern Tofua Arc (Ewart et al., 1973) and the voluminous seamount volcanism that characterized the early history of the Lau backarc basin (Bednarz and Schmincke, this volume; Clift and Dixon, this volume) also argue against a continuation of arc volcanism adjacent to the Tonga Platform throughout the rifting period. The ash record at Site 840 furthermore records a minimum, partially in the form of a sedimentary hiatus, between 5.0 and 3.0 Ma (Tappin et al., this volume; Clift and Dixon, this volume). Figure 5 graphically shows the absence of any chemical data from the 5.0–3.0 Ma interval, corresponding to the hiatus in arc magmatism. The volcanoclastic hiatus is interpreted as the time between the rifting of the original Tonga Arc and the start of activity on the new Tofua Arc, during which time volcanic activity was concentrated in the Lau Basin, and to a lesser extent on the remnant Lau Ridge (Gill, 1976). Of note is the fact that the 3.0 Ma birth of the Tofua Arc is considerably older than previous estimates, such as 1.0 Ma (Hawkins et al., 1984).

Geochemical Variations

The volcanic glass chemistry at Site 840 does have a number of features that remain constant throughout the time sampled by drilling. The glasses are consistently tholeiitic in character when plotted on an alkali/iron/magnesium (AFM) diagram (Fig. 6). The low degree of alteration of the glass permits some confidence in the AFM diagram, despite some loss of alkalis, because of glass hydration and volatilization under the electron probe beam. Chemical analysis of the basaltic andesite grains at Site 840 using ion microprobe technology (Clift and Dixon, this volume) allowed the determination of REE and trace element concentrations to the parts per million level. Not surprisingly, the basaltic and basaltic andesite glasses showed a rare-earth and trace element pattern similar to that of a normal island-arc tholeiite. Spider diagrams (Pearce, 1983) with elemental concentrations normalized against N-MORB (Sun and McDonough, 1989) show the enrichment in LILEs and marked Nb depletion that is typical of lavas generated in subduction settings (Fig. 7). Nevertheless, important trends are identifiable in the REE and trace element chemistry that show coherent changes with time. In particular, the behavior of certain critical elemental groups can provide important information about changes in the sub-arc asthenosphere and the nature of the rifting process at depth. The ratio of those elements compatible in mantle phases with those incompatible in the mantle provides a measure of the degree of depletion

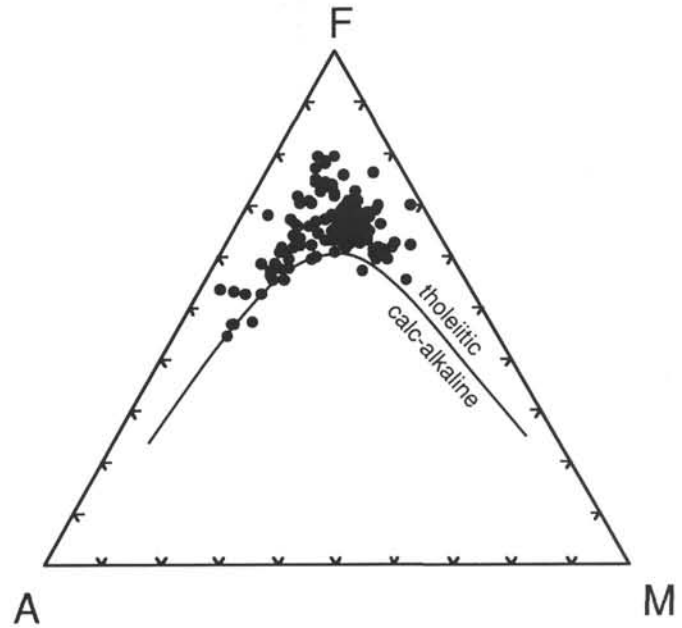


Figure 6. AFM diagram for glass grains from Sites 840 showing that the vast majority fall within the tholeiite field, as defined by Irvine and Barager (1971).

or enrichment within each elemental group. The degree of enrichment of the magma is, in turn, controlled by the degree of depletion of the source mantle and the degree of partial melting of that source. Of particular interest are the REEs, the HFSEs, and the LILEs. As the HFSEs are not considered to be affected by aqueous fluids, such as those derived from the dewatering subducting slab, their enrichment is used as a monitor of the sub-arc asthenospheric wedge. Enrichment of the HFSEs is modeled by the ratio Nb/Zr.

In view of the low concentrations of Nb (<1 ppm) in some specimens, concern arises as to the reliability of Nb/Zr as a monitor of HFSE depletion. However, Figure 8 demonstrates that, when Nb is plotted vs. Zr, a straight line correlation is achieved. The correspondence between the two is all the more impressive, as estimated counting statistic errors suggested that Nb would not be reliable below concentrations of 0.4 ppm. The Nb data from Site 840 show that high-resolution ion microprobe methods can be used with confidence to determine low elemental concentrations within single grains in ash layers. This has important implications for studies of marine ash layers worldwide.

Figure 9 shows the variation in Nb/Zr with time. A clear progression is visible toward decreasing values between 7.1 and 5.0 Ma, followed by a less well-defined trend to increasing values from 3.0 Ma to the present. This indicates increasing levels of HFSE depletion up to the point of Lau Basin rifting, followed by increasing enrichment since the start of activity of the Tofua Arc. This, in turn, indicates increasing degrees of partial melting in the mantle wedge before arc rifting, or increasing degrees of depletion of the mantle wedge source, or both. In the case of increasing degrees of partial melt, this might be achieved in an arc environment because of thinning of the arc lithosphere, which allows the sub-arc asthenosphere to upwell to shallower levels. This would increase the height of the melting column and thus produce a larger total degree of partial melt, as rifting progressed (McKenzie and Bickle, 1988). The subsequent trend to enrichment of HFSEs would then reflect thickening of the arc lithosphere by magmatic underplating of the new Tofua Arc after 3.0 Ma. Increasing source depletion is less likely as an explanation of the increasing depletion before arc rifting, but it might develop if a certain volume of mantle had several batches of melt extracted from it. This would occur if asthenospheric circulation under the arc stagnated before rifting.

In the case of the REEs, their relative depletion or enrichment can be traced by the use of the ratio La/Sm, representing light REEs/heavy

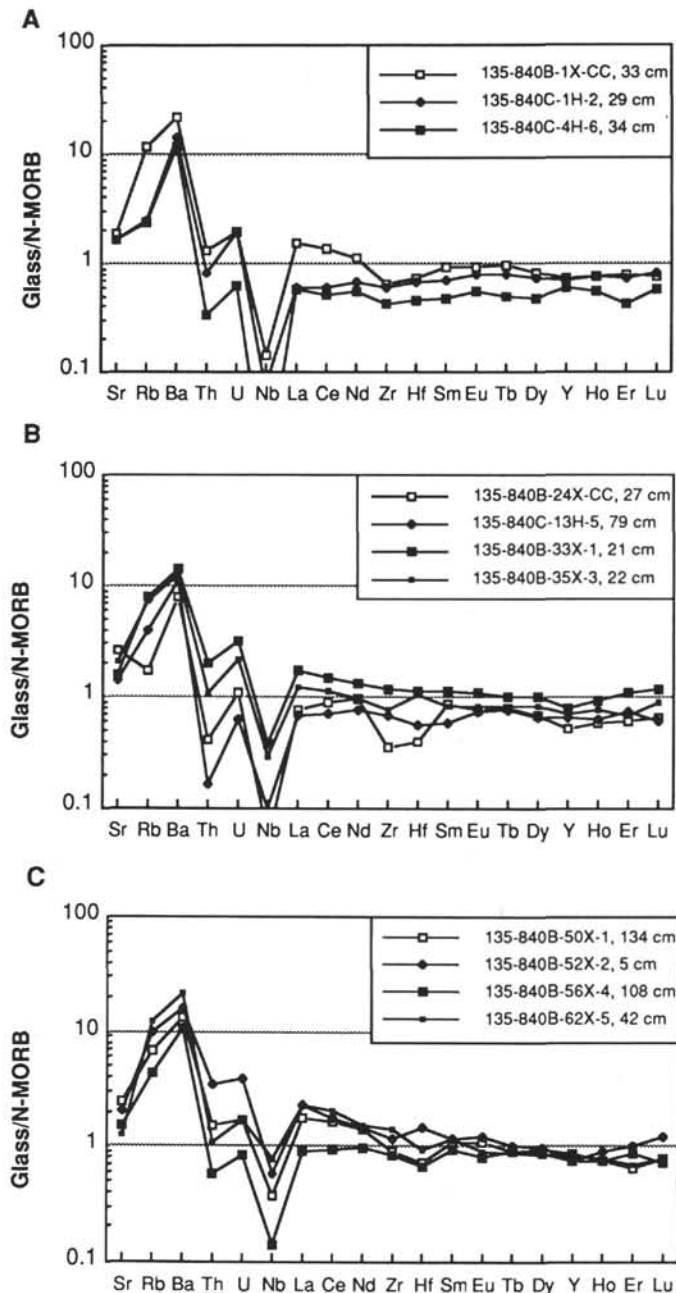


Figure 7. Spider diagrams of basaltic glass grains from Site 840, showing the subduction zone enrichment in mobile elements and the depletion in Nb. Note the consistent shape of the diagrams throughout the period of arc rifting and basin formation. **A.** Late Miocene. **B.** Uppermost late Miocene. **C.** Late Pliocene–middle Pleistocene. Elements are normalized to the N-MORB values of Sun and McDonough (1989).

REEs. Figure 9 shows the variation La/Sm over time; like the HFSEs, the trend is toward decreasing values up to the time of Lau Basin rifting. After basin rifting, the REEs show a trend toward increasing LREE enrichment with time, especially since 1.0 Ma. The similarity of this pattern to that of the HFSEs suggests that whatever is controlling the depletion or enrichment of the HFSEs is also controlling the REEs. This is an important observation as previous workers (e.g., Pearce, 1983) have suggested that light REE enrichment in arc-volcanic rocks could be caused by components added by aqueous fluids derived from the subducting slab. However, the results from Site 840 indicate that in Tonga no difference exists between the behavior of the HFSEs and

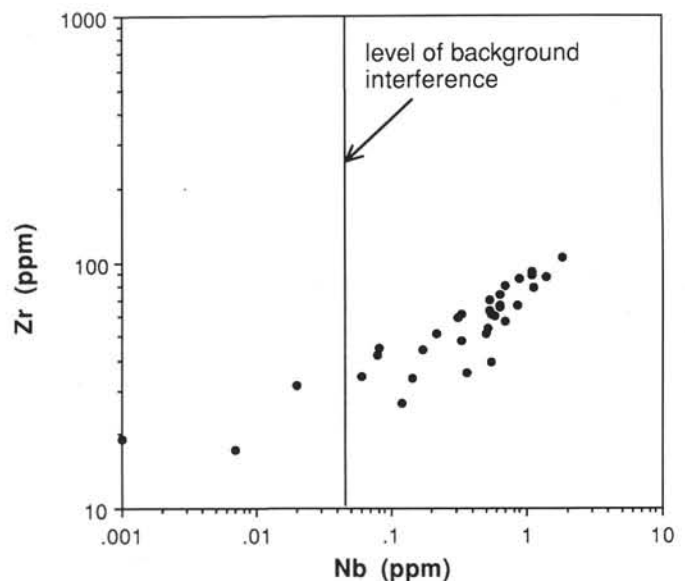


Figure 8. Covariation diagram showing the excellent correlation of Nb with Zr, even at Nb concentrations below 0.5 ppm.

the REEs, and that all variation can be accounted for by melting processes in the asthenosphere below the arc.

Variations in the flux of aqueous fluids from the subducting lithospheric slab can be gauged, however, by an examination of the changes in the LILE enrichment, as these are all water-mobile elements. Figure 9 shows that the trend to increasing depletion with time before arc rifting is also seen in the LILEs (as measured by Ba/Sr). This confirms that slab flux was insignificant in the melt generation process during this time period. It is noteworthy, however, that after 5.0 Ma the trend to increasing enrichment is more pronounced than is the case for REEs and HFSEs, with Ba/Sr far exceeding its pre-rift maximum value by 0.5 Ma. In comparison, La/Sm and Nb/Zr attain values after rifting comparable with their pre-rift values. This is the first indication that slab flux has shown a steady increase since arc rifting. Figure 10 reinforces this suggestion by showing variations in Ba/Zr with time at Site 840 and in the backarc basin (Sites 834–839). Because Ba is a LILE and Zr is a water-immobile HFSE, this ratio shows the temporal variation of water-mobile elements with time. The most important point to note is that, although a wide range of values are seen in the post-rift period (5.0 Ma to present), the maximum values are seen to be consistently low before rifting and show a progressive increase with time. This data from sediments at Site 840 and throughout the arc system strongly suggests increasing slab flux in the arc volcanism since arc rifting.

Thus, the volcanoclastic sediments from Site 840 indicate a significant change in the volume and chemistry of island-arc volcanism up to and after the time of Lau Basin rifting. A hiatus in volcanic activity between 5.0 and 3.0 Ma is preceded by a changeover from volcanism with a full range of silica contents, but dominated by dacite to a bimodal volcanism. Increasing depletion in HFSEs before rifting may indicate increasing degrees of partial melting caused by thinning of the arc lithospheric mantle before final rifting. The REEs and LILEs also show the same trend to increasing depletion before rifting and do not support an enrichment in the LREE content of the arc volcanics from the dewatering subducting slab. The LILE enrichment between 3.0 Ma and the present may be linked to increasing aqueous fluid flux from the subducting slab since rifting. The recognition of trends within volcanoclastic sediments in itself implies that the sediments of the Tonga forearc do record changes in the arc volcanism and that, consequently, the time delay between eruption of volcanic material and its reworking onto the forearc is geologically insignificant. This may be important to the interpretation of ancient volcanoclastic sequences.

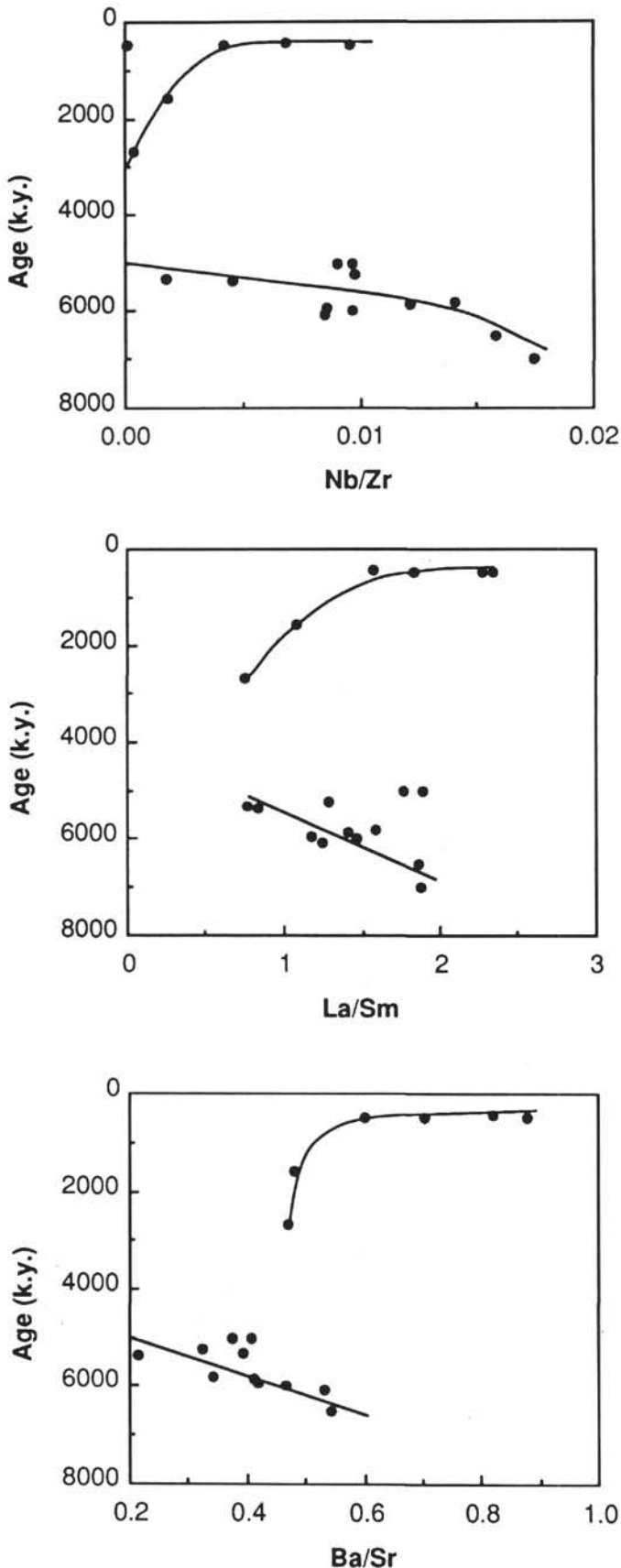


Figure 9. Diagrams showing the similar temporal variation in Nb/Zr, La/Sm, and Ba/Sr at Site 840. Note trend to increasing depletion before 5.0 Ma, followed by a poorly defined trend to increasing enrichment from 3.0 Ma to the present day.

CONCLUSIONS

Tonga Arc (Site 840)

Volcaniclastic turbidites and mass flows at Site 840 were deposited in the forearc basin of the Tonga Arc, probably on a slope that built out eastward from the volcanic front and across the forearc. Thinning and fining of individual turbidite beds upward through this basal sequence probably reflects reduced sediment supply and a change from large to smaller volume flows. Decreasing volcanic activity before arc rifting is inferred from a decrease in the coarse-grained volcaniclastic content in the upper part of the basal series (Unit III).

Increased influx of coarse-grained detrital sediments at about 5.25 Ma correlates with the initiation of rifting of the Lau Basin. This influx may be partially tectonically triggered, but it is probably also related to a peak in the intensity of high silica volcanism. Following this peak, the rapid fining of the sediments indicates a hiatus in volcanism adjacent to Site 840 between 5.0 and 3.0 Ma.

Arc rifting is preceded by uplift of the Tonga Platform and followed by subsidence. The degree and timing of the uplift is controversial. In one scenario, a modest uplift of <300 m at 6.0 Ma created the Horizon A disconformity, which was then followed by rapid, then more gentle, subsidence as the arc rifted (5.25 Ma) and the Lau Basin opened. Alternatively, a major rapid uplift of about 2000 m occurred before the breakup at 5.2 Ma and continued until after 5.1 Ma, when the Tonga Platform began to gently subside. The formation of Horizon A predates a rapid uplift by 0.9 m.y. and must represent an earlier stage of the pre-rift uplift (Fig. 11).

The Tofua Arc has been active since 3.0 Ma in its current position close to Site 840, although it may have initiated earlier further north.

Geochemical analyses of detrital glass grains show compositions lying mainly in the low-K tholeiite field, with a compositional range from basalt to rhyolite. There is a trend to decreasing scatter of higher alkali contents before arc rifting. A coherent tholeiitic trend may indicate derivation from a single volcanic source situated on the rifted part of the Lau-Tonga Ridge, possibly within the present Lau Basin. The initial opening of the Lau Basin may have been at about 6.0 Ma, although thinning of the arc lithosphere, as recorded by the trace-element depletion of single grains, dates from at least 7.0 Ma.

The volume of volcaniclastic material deposited at Site 840 after the initiation of rifting in the Lau Basin decreases markedly, which

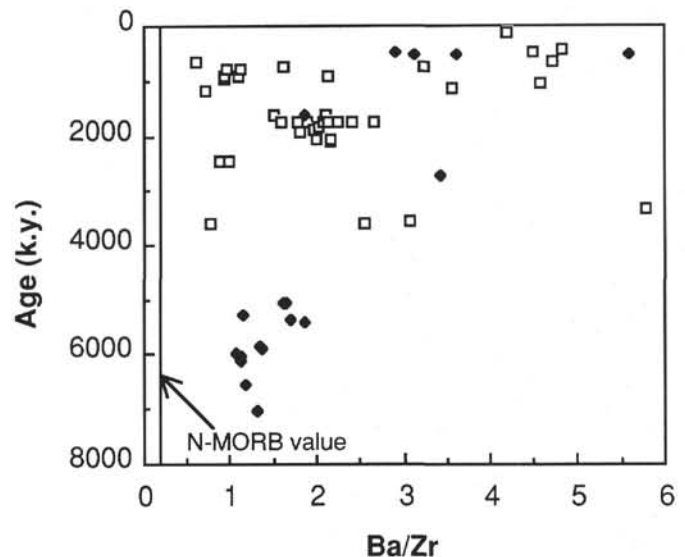
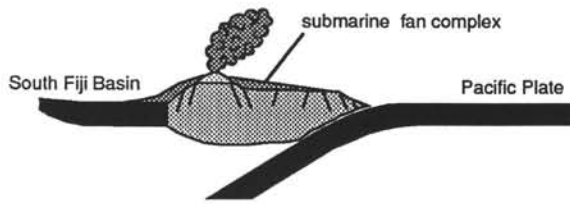


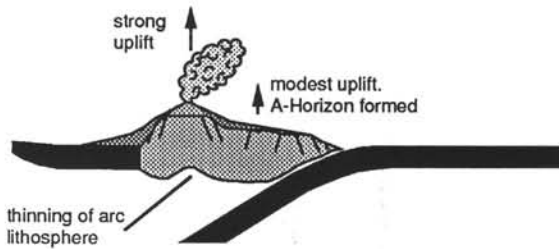
Figure 10. Diagram showing the increasing flux of slab-derived, water-mobile LILEs into the arc magma since Lau Basin rifting at 5.0 Ma as measured by Ba/Zr. Solid diamond symbols represent analyses from Site 840; square symbols represent analyses from the Lau Basin (Sites 834-839).

A

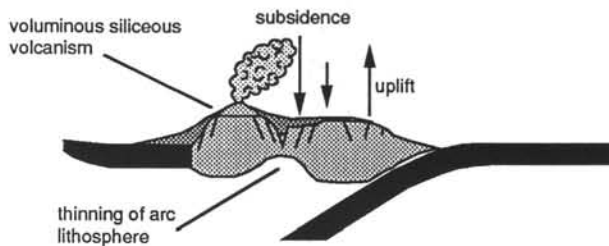
10.0 Ma: Steady state subduction - subduction erosion.



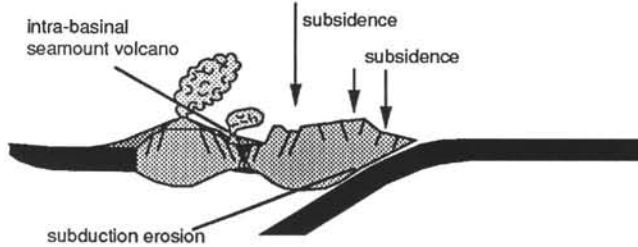
6.0 Ma: Extension of the arc



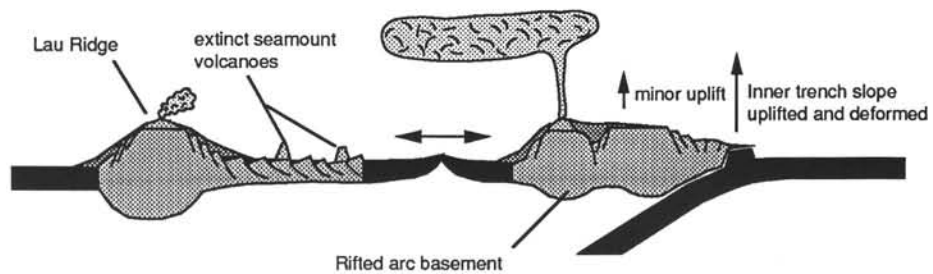
5.25 Ma: Breakup



5.0 Ma: Basin opening - sedimentary hiatus



2.0 Ma: Basin Spreading and Louisville Ridge Collision



B

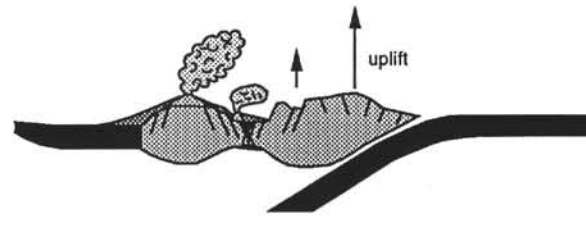
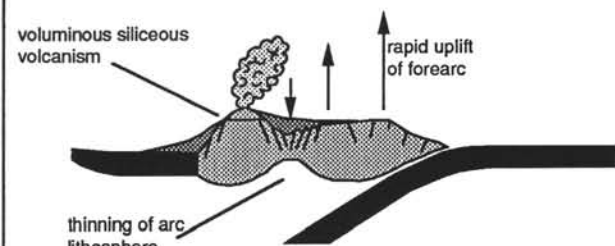
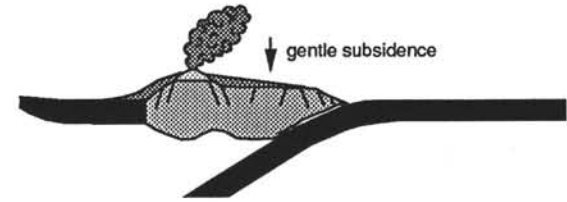
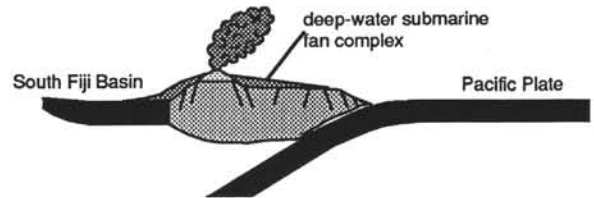


Figure 11. Diagrams showing the two alternative tectono-sedimentary histories for the Tonga forearc since 7.0 Ma. **A.** Model of Clift (this volume) and Tappin et al. (this volume). **B.** Model of Ledbetter and Haggerty (this volume) and Dupont and Herzer (1985). Relative magnitude of uplift and subsidence is indicated by the length of the arrows.

may reflect the cessation of arc activity on the east side of the basin between 5.0 and 3.0 Ma.

Trace and rare-earth-element analyses indicate increasing depletion with time in HFSEs, REEs, and LILEs in basaltic glass grains before Lau Basin rifting. This may be the result of a stagnation of asthenospheric circulation under the arc, but most probably it is the result of thinning of the arc lithosphere before the opening of the Lau Basin. After basin rifting, there is a trend to HFSE, REE, and LILE enrichment because of magmatic underplating of the new Tofua Arc. In addition, enhanced LILE enrichment indicates the increasing influence of the subducting slab since 3.0 Ma.

No sedimentary response or evidence of a change in paleowater depth is present within the range of uncertainty (300–600 m) at either Sites 840 or 841 during the collision of the Louisville Ridge with that section of the trench.

Tonga Forearc (Site 841)

Three episodes of sedimentation have been identified at Site 841: one initiated at 37.0, another before 16.0 Ma, and a third at 10.0 Ma. Sedimentation at 37.0 Ma reflects a rapid deepening episode within the outer forearc basin and is contemporaneous with the rifting of the South Fiji Basin. Packages of coarse clastic sediments deposited between 16.0 and 14.0 Ma and between 10.0 Ma and the Holocene occur as two upward-fining cycles. Sediments deposited between 35.0 and 16.0 Ma were eroded away immediately before the start of high-energy, mass-flow sedimentation at 16.0 Ma. A cycle of sedimentation from 16.0 to 14.0 Ma does not correlate with a known tectonic event but may be related to extensional faulting caused by subduction erosion of the forearc. Normal faulting has removed the sedimentary record from 14.0 to 10.0 Ma. However, fining-upward sedimentation dating from at least 10.0 Ma approximately correlates with the initiation of subduction along the New Hebrides Arc immediately to the west, and may have been caused by extension and rotation of the arc caused by changes in plate boundary stresses. Sediment influx at 16.0 and 10.0 Ma may also be related to major falls in eustatic sea level increasing erosion of the arc edifice. Both events correlate well with the sea-level curve of Haq et al. (1987), although other predicted falls and rises are not recorded at Site 841.

ACKNOWLEDGMENTS

We thank the Shipboard Scientific Party, the ODP technicians, and the SEDCO drilling crew of Leg 135. We also thank U. von Rad for generously providing unpublished XRF data of volcanoclastic sediments recovered during *Sonne* cruises.

REFERENCES*

- Austin, J.A., Taylor, F.W., and Cagle, C.D., 1989. Seismic stratigraphy of the central Tonga Ridge. *Mar. Pet. Geol.*, 6:71–92.
- Berger, W.H., Ekdale, A.A., and Bryant, P.P., 1979. Selective preservation of burrows in deep-sea carbonates. *Mar. Geol.*, 32:205–230.
- Bouma, A.H., 1962. *Sedimentology of Some Flysch Deposits: A Graphic Approach to Facies Interpretation*. Amsterdam (Elsevier).
- Cawood, P.A., 1991. Nature and record of igneous activity in the Tonga arc, SW Pacific, deduced from the phase chemistry of derived detrital grains. In Morton, A.C., Todd, S.P., and Haughton, P.D.W. (Eds.), *Developments in Sedimentary Provenance Studies*. Geol. Soc. Spec. Publ. London, 57:305–321.
- Dupont, J., and Herzer, R.H., 1985. Effect of subduction of the Louisville Ridge on the structure and morphology of the Tonga arc. In Scholl, D.W., and Vallier, T.L. (Eds.), *Geology and Offshore Resources of Pacific Island Arcs—Tonga Region*. Circum-Pac. Council. Energy Mineral Resour., Earth Sci. Ser., 2:323–332.

- Einsele, G., 1991. Submarine mass flow deposits and turbidites. In Einsele, G., Ricken, W., and Seilacher, D. (Eds.), *Cycles and Events in Stratigraphy*. Berlin (Springer-Verlag), 313–339.
- Ekdale, A.A., Bromley, R.G., and Pemberton, S.G. (Eds.), 1984. *Ichthyology: Trace Fossils in Sedimentology and Stratigraphy*. SEPM Short Course, 15.
- Ekdale, A.A., Muller, L.N., and Novak, M.T., 1984. Quantitative ichthyology of modern pelagic deposits in the abyssal Atlantic. *Palaeogeogr., Palaeoclimatol., Palaeoecol.*, 45:189–223.
- Ewart, A., Bryan, W.B., and Gill, J., 1973. Mineralogy and geochemistry of the younger volcanic islands of Tonga, southwest Pacific. *J. Petrol.*, 14:429–465.
- Gill, J.B., 1976. Composition and age of Lau basin and ridge volcanic rocks: implications for evolution of an interarc basin and remnant arc. *Geol. Soc. Am. Bull.*, 87:1384–1395.
- Haq, B.U., Hardenbol, J., and Vail, P.R., 1987. Chronology of fluctuating sea levels since the Triassic. *Science*, 235:1156–1167.
- Hawkins, J.W., Bloomer, S.H., Evans, C.A., and Melchior, J.T., 1984. Evolution of intra-oceanic arc-trench systems. *Tectonophysics*, 102:175–205.
- Hayward, B.W., 1976. Lower Miocene bathyal and submarine canyon ichno-coenoses from Northland, New Zealand. *Lethaia*, 9:149–62.
- Herzer, R.H., and Exon, N.F., 1985. Structure and basin analysis of the southern Tonga forearc. In Scholl, D.W., and Vallier, T.L. (Eds.), *Geology and Offshore Resources of Pacific Island Arcs—Tonga Region*. Circum-Pac. Council. Energy Mineral Resour., Earth Sci. Ser., 2:55–73.
- Irvine, T.N., and Barager, W.R., 1971. A guide to the chemical classification of common igneous rocks. *Can. J. Earth Sci.*, 8:523–548.
- Keen, C.E., 1985. The dynamics of rifting: deformation of the lithosphere by active and passive driving forces. *Philos. Trans. R. Soc. London*, 80:95–120.
- McKenzie, D.P., and Bickle, M.J., 1988. The volume and composition of melt generated by extension of the lithosphere. *J. Petrol.*, 29:625–679.
- Moberly, R., 1971. Youthful oceanic lithosphere of marginal isles, western Pacific. *Proc. 12th Pac. Sci. Congr.*, Canberra.
- Nishimura, A., Marsaglia, K.M., Rodolfo, K.S., Colella, A., Hiscott, R.N., Tazaki, K., Gill, J.B., Janecek, T., Firth, J., Isiminger-Kelso, M., Herman, Y., Taylor, R.N., Taylor, B., Fujioka, K., and Leg 126 Scientific Party, 1991. Pliocene-Quaternary submarine pumice deposits in the Sumisu rift area, Izu-Bonin arc. In Fisher, R.V., and Smith, G.A. (Eds.), *Sedimentation in Volcanic Settings*. Spec. Publ.—Soc. Econ. Paleontol. Mineral., 45:201–208.
- Packham, G.H., 1978. Evolution of a simple island arc: the Lau-Tonga Ridge. *Aust. Soc. Expl. Geophys. Bull.*, 9:133–140.
- Parson, L., Hawkins, J., Allan, J., et al., 1992. *Proc. ODP, Init. Repts.*, 135: College Station, TX (Ocean Drilling Program).
- Pearce, J.A., 1983. The role of sub-continental lithosphere in magma genesis at active continental margins. In Hawkesworth, C.J., and Norry, M.J. (Eds.), *Continental Basalts and Mantle Xenoliths*. Nantwich (Shiva Publ.), 230–249.
- Slater, J.G., and Christie, P.A.F., 1980. Continental stretching: an explanation of the post-mid-Cretaceous subsidence of the central north sea basin. *J. Geophys. Res.*, 85:3711–3739.
- Scholl, D.W., Vallier, T.L., and Packham, G.H., 1985. Framework geology and resource potential of the southern Tonga platform and adjacent terranes—a synthesis. In Scholl, D.W., and Vallier, T.L. (Eds.), *Geology and Offshore Resources of Pacific Island Arcs—Tonga Region*. Circum-Pac. Council. Energy Mineral Resour., Earth Sci. Ser., 2:457–488.
- Stow, D.A.V., and Shanmugam, G., 1980. Sequences of structures in fine-grained turbidites: comparison of recent deep-sea and ancient flysch sediments. *Sediment. Geol.*, 25:23–42.
- Sun, S.-S., and McDonough, W.F., 1989. Chemical and isotopic systematics of oceanic basalts: implications for mantle composition and processes. In Saunders, A.D., and Norry, M.J. (Eds.), *Magmatism in the Ocean Basins*. Geol. Soc. Spec. Publ. London, 42:313–345.
- Taylor, B., 1992. Rifting and the volcanic-tectonic evolution of the Izu-Bonin-Mariana Arc. In Taylor, B., Fujioka, K., et al., *Proc. ODP, Sci. Results*, 126: College Station, TX (Ocean Drilling Program), 627–651.
- van Andel, T.H., 1975. Mesozoic-Cenozoic calcite compensation depth and the global distribution of calcareous sediments. *Earth Planet. Sci. Lett.*, 26:187–194.
- Weissel, J.K., and Watts, A.B., 1975. Tectonic complexities in the south Fiji marginal basin. *Earth Planet. Sci. Lett.*, 28:121–126.

Date of initial receipt: 17 May 1993

Date of initial acceptance: 30 June 1993

Ms 135SR-164

* Abbreviations for names of organizations and publication titles in ODP reference lists follow the style given in *Chemical Abstracts Service Source Index* (published by American Chemical Society).